JAST (Journal of Animal Science and Technology) TITLE PAGE

Upload this completed form to website with submission

ARTICLE INFORMATION	Fill in information in each box below
Article Type	Research article
Article Title (within 20 words without abbreviations)	Protective effects of enzymatically digested velvet antler polypeptides on mitochondria in primary astrocytes
Running Title (within 10 words)	Effects of enzymatically digested VA extract on astrocytes
Author	Yunn Me Me Paing1 and Sung Hoon Lee1
Affiliation	1 College of Pharmacy, Chung-Ang University, 84 Heukseok-ro, Dongjak-gu, Seoul 06974, Republic of Korea
ORCID (for more information, please visit https://orcid.org)	Yunn Me Me Paing (https://orcid.org/0000-0003-4116-9534) Sung Hoon Lee (https://orcid.org/0000-0002-1805-8281)
Competing interests	No potential conflict of interest relevant to this article was reported.
Funding sources State funding sources (grants, funding sources, equipment, and supplies). Include name and number of grant if available.	Not applicable.
Acknowledgements	We thank Dr. Yusuke Ohba (Tom20) and Dr. Gia Voeltz (Drp1 and Mfn2) for providing the plasmids. We also thank Yuhan Care Co., Ltd for providing YC-1101 and YHC-BE-2038.
Availability of data and material	Upon reasonable request, the datasets of this study can be available from the corresponding author.
Authors' contributions Please specify the authors' role using this form.	Conceptualization: Lee SH. Formal analysis: Paing YMM. Investigation: Paing YMM. Writing - original draft: Paing YMM. Writing - review & editing: Paing YMM. Lee SH.
Ethics approval and consent to participate	The animal experiments were approved by the Institutional Animal Care and Use Committee of Chung-Ang University (2020-00049).

CORRESPONDING AUTHOR CONTACT INFORMATION

For the corresponding author (responsible for correspondence, proofreading, and reprints)	Fill in information in each box below
First name, middle initial, last name	Sung Hoon Lee
Email address – this is where your proofs will be sent	sunghoonlee@cau.ac.kr
Secondary Email address	Imperator308@gmail.com
Address	Chung-Ang University, Seoul 06974, Republic of Korea
Cell phone number	821045460124
Office phone number	8228205675
Fax number	8228150054

Abstract

Traditionally, velvet antler (VA) has been used as a medicine or dietary supplement in East Asia. It contains biologically active compounds that exert anti-inflammatory, anti-fatigue, anti-aging, and anticancer effects. Although demand for VA has increased globally, its supply and consumption are limited due to the low recovery of its bioactive compounds from traditional decoctions. Therefore, alternative extraction methods are required to enrich the active compounds and enhance their biological efficacy. The extract has been reported to protect against neuropathological conditions in brain cells and suppress oxidative stress and neuroinflammation—crucial for the initiation or progression of neurodegenerative diseases. Therefore, VA is a potential therapeutic agent for neurodegenerative diseases. However, the beneficial effects of VA on astrocytes, which are the predominant glial cells in the brain, remain unclear. In the present study, we investigated the protective effects of enzymatically digested VA extract (YC-1101) on the mitochondria in astrocytes, which are essential organelles regulating oxidative stress. Proteomic and metabolomic results using LC-MS/MS identified enriched bioactive ingredients in YC-1101 compared to hot water extract of VA. YC-1101 displayed significant protective effects against mitochondrial stressors in astrocytes compared with other health functional ingredients. Altogether, our results showed improved bioactive efficacy of YC-1101 and its protective role against mitochondrial stressors in astrocytes.

Keywords (3 to 6): Velvet extract, enzymatic digestion, mitochondria, lipopolysaccharide, scopolamine, primary astrocytes

Introduction

Velvet antler (VA) has been used as a traditional medicine in East Asia for thousands of years to treat mammary hyperplasia, immune dysfunction, cardiovascular diseases, cancer, and gynecological problems [1]. Previous studies have reported that VA has bioactive properties including anti-inflammatory, anti-aging, and anti-fatigue effects, as well as, being known to strengthen the muscles and bones [2]. In addition, VA is consumed as a dietary supplement in the form of dried slices or as medicinal soup in several regions, including East Asia, the USA, Canada, and New Zealand [3]. Although the global production of VA is rapidly growing to meet the medicinal market demands for older adults [4], its supply and consumption are limited. The traditional formulation of VA is a decoction or medicinal liquor using hot water; however, hot water used for extraction possibly denatures bioactive compounds and reduces their pharmacological efficiency [3]. In addition, extraction using organic solvents is restricted to the

food industry [5]. Enzymatic methods are now being increasingly used to study the efficacy and enrich the bioactive compounds of VA [6].

Astrocytes are the predominant glial cells implicated in several brain functions and diseases. Astrocytes maintain the central nervous system (CNS) homeostasis by controlling synapses, neurotransmitters, ions, water, and pH in the brain [7]. In addition, astrocytes undergo morphological changes and regulate neuroinflammation in response to the release of pro-inflammatory mediators during aging, injury, and pathological conditions. The mitochondria in astrocytes have been reported to be involved in several physiological conditions, such as generation of ATP, regulation of oxidative stress and neuroinflammation response [8], fatty acid metabolism [9], transmitophagy [10], and controlling glutamate metabolism [11] and intracellular Ca2+ concentration [12]. Disruption of mitochondrial functions in astrocytes can inactivate or activate the astrocytes, which initiates or aggravates neurodegenerative diseases [13].

Mitochondria are interconnected structures with a negative membrane potential inside the mitochondrial matrix. They provide an electrochemical proton gradient for ATP production and reactive oxygen species (ROS) formation via oxygen reduction. Mitochondrial morphology and mitochondrial membrane potential (MMP) are intricately related to mitochondrial functions and share reciprocal interrelationships. Mitochondrial size is associated with MMP, oxidative stress, and ATP production [14, 15]. Conversely, MMP is required for the regulation of mitochondrial morphology and superoxide formation [16]. In addition, deficiency of mitofusin (Mfn)2, a mitochondrial fusion factor, reduces MMP. Conversely, loss of MMP causes abnormal mitochondrial morphology by regulating optic atrophy 1 (OPA1), a mitochondrial fusion protein [17]. In the present study, we investigated the effects of the enzymatically digested VA extract on mitochondrial characteristics, including mitochondrial morphology, mitochondrial superoxide, and MMP, in primary astrocytes treated with mitochondrial stressors such as lipopolysaccharide (LPS) or scopolamine.

Materials and Methods

Materials and reagents

Lipopolysaccharide (LPS, 10 ng/mL) serotype 055:B5 was purchased from Merck (St. Louis, MO, USA), and its concentration was determined as previously described [18]. Scopolamine (2 mM) was purchased (Merck), and its concentration was determined as previously described [19].

Preparation of compounds

YC-1101 (HENKIV® , deer velvet [Cervus elaphus L.]) and YHC-BE-2038 were obtained from Yuhan Care Co., Ltd. (Seoul, Korea). To prepare YC-1101, the freeze-dried powder obtained from New Zealand was mixed with water and flavourzyme (Daejongzymes, Seoul, Korea). YHC-BE-2038 was prepared by excluding the enzyme decomposition process [20]. Red ginseng extract was purchased as red ginseng concentrate from the Gimpo Paju Ginseng Agricultural Cooperative (Paju, Republic of Korea). This extract contained the ginsenosides Rg1, Rb1, and Rg3. AGCP (Angelica gigas Nakai, Cnidium officinale Makino and Paeonia lactiflora Pallas) was a freeze-dried extract purchased from Atomy HemoHIM (Gongju, Korea). Aloe gel extract was provided by AMB Wellness (Gómez Palacio, Durango, Mexico) and had a total polysaccharide content > 10%. Beta-glucan and ginsenoside compound K were purchased from Merck.

Sample preparation for proteomic and metabolomic analyses

YC-1101 and YHC-BE-2038 samples were sonicated using a focused ultrasonicator (Covaris S-Series, Covaris Inc., Woburn, MA, USA) with Adaptive Focused Acoustics in 8 M urea to extract the proteome. The protein concentration of the samples was measured using the Pierce bicinchoninic acid (BCA) Protein Assay Kit (Thermo Scientific, Rockford, IL, USA). Next, 200 μg of the protein sample was mixed with 100 μL of 0.1 M Tris-HCl containing 8 M urea at pH 8.5 in a 1.5 mL Eppendorf tube. Denatured protein was reduced with 1 μL of 500 mM Tris(2-carboxyethyl)phosphine (TCEP) (Thermo Fisher Scientific) for 20 min at 37°C and 900 rpm. Subsequently, the sample was alkylated with 3 μL of 500 mM iodoacetamide (Merck) for 30 min at 25°C and 300 rpm in the dark. The protein sample was digested with sequencing-grade modified trypsin (Promega, WI, USA) at an enzyme:protein ratio of 1:20 (w/w) at 47°C. The peptides were desalted using Sep-Pak Vac 1 cm3 (50 mg) C18 cartridges (Waters Corporation, Milford, MA, USA) and subsequently dried using SpeedVac (Bio-Rad, Hercules, CA, USA).

For metabolomic analysis, YC-1101 was incubated in water at 4°C for 10 min and precipitated with 80% methanol. Following that, the mixture was centrifuged at 2,000 rpm for 10 min. The supernatant was transferred to an Eppendorf tube and dried using a SpeedVac.

Liquid chromatography–mass spectrometry (LC-MS)/MS analysis

Before liquid chromatography–mass spectrometry (LC-MS)/MS proteomic analysis, dried samples were re-suspended in 50 μL of 0.1% formic acid, and 1 μg of peptides from the sample was injected into the Acclaim PepMap™ 100 C18 nano-trap column (3 μm, 100 Å, 75 μm × 2 cm) at a flow rate of 2.5 μL/min for 5 min in 0.1% formic acid. The peptides were separated using a PepMap™ RSLC C18 nano-column (2 μm, 100 Å, 75 μm × 50 cm) at a flow rate of 300 nL/min. Analysis was performed with a Q-Exactive orbitrap hybrid mass spectrometer along with an Easy nano-ESI-LC 1000 system (Thermo Fisher Scientific). The mobile phase consisted of water containing 0.1% formic acid (v/v, solvent A) and 0.1% formic acid in acetonitrile (v/v, solvent B). The gradient was set linearly as follows: holding at 4% solvent (B) for 14 min, from 4% to 40% solvent (B) for 136 min, from 40% to 96% solvent (B) for 0.1 min, holding at 96% solvent (B) for 9.9 min, from 96% to 4% solvent (B) for 0.1 min, and equilibrating the column with 4% solvent (B) for 19.9 min.

For LC-MS/MS analysis of the metabolites, the dried sample was dissolved in 100 μL of 0.1% formic acid in water. The solution was injected into an Eclipse Plus C18 RRHD column (1.8 μm, 50 mm × 2.1 mm) at a flow rate of 200 μL/min, and the analysis was performed using a Q-Exactive orbitrap hybrid mass spectrometer with an Easy nano-ESI-LC 1000 system (Thermo Fisher Scientific). The mobile phase consisted of water containing 0.1% formic acid (v/v, solvent A) and 0.1% formic acid in 80% acetonitrile (v/v, solvent B). The gradient was set up linearly as follows: 2.5% solvent (B) for 5 min, 2.5% to 12.5% solvent (B) for 29 min, 12.5% to 25% solvent (B) for 11 min, 25% to 37.5% solvent (B) for 11 min, 37.5% to 80% solvent (B) for 17 min, 80% to 2.5% solvent (B) for 0.1 min and equilibration of the column at 4% solvent (B) for 2.5 min.

Data-dependent acquisition was adopted, and the top 10 precursor peaks were first fragmented with higher-energy collisional dissociation and 27 others with normalized collisional energies. The following MS/MS setup parameters were used: ionization mode, positive ion electrospray; spray voltage, +2.0 kV; capillary temperature, 270°C; S-lens, +55 V; and isolation width, ± 3 Da. Ions were scanned at a high resolution (70,000 in MS1, 17,500 in MS2 at m/z 400), and the MS scan range was 150 to 1000 m/z (proteomic analysis) or 400 to 2000 m/z (metabolite analysis) at both MS1 and MS2 levels. A dynamic exclusion time of 30 s was set to minimize the repeated analyses of the same precursor ions.

Proteomic and metabolomics data analyses

Raw MS/MS data files were first converted to the mzXML format using an MSConverter and subsequently analyzed with Comet (Version 2016.01 rev.2) against the UniProt cervus+elaphus FASTA file. The identification settings were as follows: trypsin with a maximum of two missed cleavages; 10 ppm precursor mass tolerance and 0.02 Da fragment mass tolerance; variable modifications: oxidation of methionine (+15.995 Da), carbamylation of protein N-terminus (+43.006 Da), and carbamidomethylation of cysteine. The search results in the pepXML format were imported into the trans-proteomic pipeline (TPP). In the TPP, a cut-off probability score of 0.95 was used for this work. It revealed a ≤ 1% peptide false discovery rate (FDR) based on a PeptideProphet probability cut-off score of 0.95. ProteinProphet infers the simplest list of proteins consistent with the peptides identified for protein-level validation and final inference.

The MS/MS data files were analyzed using Compound Discoverer 3.1.1.12. Raw data were analyzed in untargeted metabolomics with statistics detecting unknown compounds with IDs using an online database and mzlogic mode. The compounds were identified using mzCloud (ddMS2) and ChemSpider software. All compounds were searched for ddMS2 data similarities using mzCloud.

Primary cortical astrocyte culture and transfection

Animals were handled according to the National Institutes of Health Guidelines for Laboratory Animal Care. The animal experiments were approved by the Institutional Animal Care and Use Committee of Chung-Ang University (2020-00049). Sprague-Dawley rat pups (postnatal day 1, weighing 7–9 g) were purchased from Young Bio (Gyeonggi-do, Republic of Korea) and used for culturing primary astrocytes following a previously described method [18]. Briefly, the cortices were dissected from the pup's brain and dissociated into cells by mechanical pipetting. Primary cultures were seeded onto poly-D-lysine (PDL, Merck)-coated T75 flasks supplemented with Dulbecco's modified Eagle's medium/nutrient mixture F12 (DMEM/F12, Thermo Fisher Scientific) containing 10% fetal bovine serum (FBS, GW Vitek, Seoul, Republic of Korea), and penicillin/streptomycin (Thermo Fisher Scientific) and grown for 7 days at 37℃ in a humidified chamber with 5% CO2. Subcultures were incubated with 0.25% trypsin-ethylenediaminetetraacetic acid, and astrocytes were grown for an additional 5 days in DMEM/F12 containing 10% FBS.

Transfection was performed on the third day of subculture using Lipofectamine LTX Reagent with PLUS™ Reagent (Thermo Fisher Scientific) supplemented with Opti-MEM (Thermo Fisher Scientific). The amount of plasmid DNA was determined according to the manufacturer's instructions. Fresh medium was added 6 h after the transfection.

150

151 Plasmids

152 Translocase of the outer membrane 20 (Tom20; Addgene plasmid #174188) was a gift from Yusuke Ohba. Drp1

153 (Addgene #49152) and mitofusin 2 (Mfn2; Addgene #141156) were gifted by Gia Voeltz.

154

155 MTT assay

156 Toxicity in primary astrocytes was determined using the 3-(4, 5-dimethylthiazol-2-yl)-2,5-diphenyltetrazolium

157 bromide (MTT) assay. Astrocytes were incubated with compounds for 24 h at the indicated concentrations and

158 treated with MTT (100 μg/mL) solution. After 1 h of incubation, the insoluble formazan blue was extracted with

159 dimethyl sulfoxide (DMSO), and the absorbance was measured using a microplate reader (BioTek Instruments, VT,

160 USA).

161

162 Imaging and analyses

163 Astrocytes seeded onto coverslips were treated with CMXRos (100 nM, Thermo Fisher Scientific) and incubated for

164 15 min at 37℃. The coverslips were fixed with 4% paraformaldehyde for 15 min and permeabilized with 0.1%

165 Triton X-100 in Dulbecco's phosphate buffered saline (DPBS) for 10 min at 15 to 25℃. Coverslips were incubated

166 in DPBS containing 1% bovine serum albumin (Merck) and anti-glial fibrillary acidic protein (GFAP) antibody

167 (Santa Cruz, TX, USA) at 4℃ overnight. Thereafter, the coverslips were washed thrice and incubated in DPBS

168 containing 1% bovine serum albumin (Merck) and Alexa Fluor 488® -conjugated secondary antibody (Abcam,

169 Cambridge, UK) for 1 h at 15 to 25℃. Coverslips were mounted using a mounting solution (Biomeda, CA, USA).

170 The mitochondrial superoxide activity was measured using MitoSOX (Thermo Fisher Scientific). MitoSOX was

171 applied to coverslips and incubated for 10 min at 37℃. After incubation, cells were rapidly washed thrice with a

172 bath solution containing 119 mM NaCl, 2.5 KCl, 25 mM HEPES (pH 7.4), 2 mM CaCl2, 2 mM MgCl2, and 30 mM

173 glucose. The coverslips were moved to a living cell chamber (Gataca Systems, France) to capture images.

174 Images were captured using a confocal microscope (LSM 800, Zeiss, Germany). The fluorescence intensity of each

175 indicator was measured in a single cell and is shown as arbitrary units (a.u.) for quantification.

176

177 Statistical analysis

Data are presented as the mean ± standard error of the mean (SEM) of three independent experiments. Data were analyzed using the Mann–Whitney *U* test for non-parametric tests or one-way analysis of variance (ANOVA), followed by *a post hoc* Tukey's test, using GraphPad Prism software (version 5.0; GraphPad Software, Inc., CA, USA). Statistical significance was set at $p<0.05$.

Results

Identification of bioactive compounds in YC-1101

VA was extracted using two different methods: traditional (using hot water) and enzymatic. YC-1101 was enzymatically digested, and YHC-BE-2038 was digested using hot water. The bioactive compounds were analyzed using LC-MS/MS. A total of 143 peptides and 44 proteins were detected in YC-1101, which were absent in YHC-BE-2038 (Fig. 1A). In addition, 23 metabolites were detected in YC-1101 using metabolomic analysis (Table 1 and Fig. 1B). These results indicated that bioactive low-molecular weight of VA peptides were enriched in enzymatically digested VA compared to the traditional water extract of VA.

Cellular toxicity of YC-1101 and other compounds in primary cultured astrocytes

We compared the effect of YC-1101 on the mitochondria in primary cultured astrocytes with that of YHC-BE-2038. Additionally, the effect of YC-1101 was also compared with several compounds known to restore mitochondria, such as red ginseng [21], AGCP [22], aloe gel [23], beta-glucan [24], and compound K [25]. Initially, the appropriate concentration of each compound was determined using the MTT assay. Primary cortical astrocytes were incubated with each compound for 24 h at 37℃ and cell viability was measured. In astrocytes, all compounds except compound K at a concentration of 0.5 mg/mL and 2 μM of compound K had not shown significant cellular toxicity (Fig. 2). Therefore, these concentrations were used for subsequent analyses.

Effects of YC-1101 on mitochondrial membrane potential in LPS- or scopolamine-treated primary astrocytes

Scopolamine and LPS are known to damage mitochondrial physiology by disrupting the mitochondrial membrane potential (MMP) and enhancing mitochondrial fragmentation and the activity of mitochondrial superoxide [26, 27]. We initially investigated the rescue effects of YC-1101 against LPS- and scopolamine-induced MMP disruption.

Primary astrocytes were first incubated with the compounds for 1 h before being incubated with LPS or scopolamine for 24 h at 37℃. The highest concentration of DMSO (0.1%) was used as the vehicle (Veh). MMP was measured by incubation with CMXRos, which is a cationic fluorescent dye that is trapped inside the mitochondrial matrix by negative MMP [28]. After fixation, the astrocytes were immunostained for glial fibrillary acidic protein (GFAP), an astrocyte marker. LPS treatment decreased the intensity of CMXRos compared to the Veh group (Fig. 3A), indicating that LPS induced the depolarization of MMP in astrocytes. Intriguingly, YC-1101 restored the LPS-induced depolarization of MMP in astrocytes; however, the restoration effect was not observed with YHC-BE-2038. These results indicated that the effectiveness of VA on mitochondria depends on the extraction method used. In addition, red ginseng, AGCP, aloe gel, beta-glucan, and compound K did not induce significant changes in MMP compared to LPS-treated astrocytes.

We further investigated the effect of YC-1101 on the MMP in scopolamine-treated astrocytes. Consistent with the LPS results, YC-1101 reversed the reduction in MMP in scopolamine-treated astrocytes (Fig. 3B). However, other compounds did not induce significant changes in MMP compared to scopolamine-treated astrocytes.

Effects of YC-1101 on mitochondrial superoxide in LPS- or scopolamine-treated astrocytes

Superoxide is primarily produced by the electron transport chain in the mitochondria, which causes mitochondrial dysfunction, cellular oxidative stress, and related diseases [29]. MitoSOX is a mitochondria-targeted fluorescent probe that is rapidly oxidized by superoxide and produces fluorescence in living cells [30]. Therefore, we investigated the effects of YC-1101 on mitochondrial superoxide production using MitoSOX in living astrocytes treated with LPS or scopolamine. LPS enhanced the intensity of MitoSOX, which was attenuated by YC-1101 treatment (Fig. 4A). Additionally, YC-1101 similarly restored MitoSOX upregulation in scopolamine-treated astrocytes (Fig. 4B). However, other compounds exhibited MitoSOX intensities that were comparable to those of LPS- or scopolamine-treated astrocytes.

Effects of YC-1101 on mitochondrial morphology in LPS- or scopolamine-treated primary astrocytes

Next, we investigated the effects of YC-1101 on mitochondrial morphology. Tom20 is expressed in the outer mitochondrial membrane, which is necessary for the transport of mitochondrial proteins [31]. Furthermore, the overexpression of Tom20 selectively displays mitochondrial morphology [32]. Astrocytes were transfected with Tom20 and treated with LPS or scopolamine, as described above. LPS induced a reduction in Tom20 staining

intensity and mitochondrial fragmentation in astrocytes, and YC-1101 rescued these LPS-induced changes in mitochondrial morphology (Fig. 5A). Similarly, YC-1101 enhanced the scopolamine-induced suppression of Tom20 expression in astrocytes (Fig. 5B). Compared to LPS- or scopolamine-treated astrocytes, other compounds did not show significant differences in Tom20 expression.

Effects of YC-1101 on mitochondrial fission and fusion factors in LPS or scopolamine-treated primary astrocytes

We investigated the effects of YC-1101 on the expression of mitochondrial fission and fusion factors. Drp1- or Mfn2-overexpressed astrocytes were treated with LPS or scopolamine. YC-1101 attenuated LPS- or scopolamine-induced elevation in Drp1-overexpressed astrocytes (Figs. 6A and B). However, LPS or scopolamine did not change the expression of Mfn2 in astrocytes, and YC-1101 showed a similar expression of Mfn2 following LPS or scopolamine treatment (Figs. 7A and B). These results indicated that YC-1101 regulates mitochondrial morphology by controlling the expression of fission factors in astrocytes. The other compounds did not induce significant changes in Drp1 or Mfn2 expression in LPS- or scopolamine-treated astrocytes.

Discussion

Several active compounds have been identified in VA, including peptides, amino acids, steroids, minerals, inorganic elements, growth factors, and other ingredients. Because bioactive proteins in organisms typically exist in an inactive state, the recovery of these proteins through conformational changes is required to achieve efficacious therapeutic effects. Although the water extraction method is common, easy, and displays biological activities, it achieves a low recovery of bioactive compounds owing to difficulties in conformational arrangements and complicated extraction [33]. Therefore, alternative extraction methods for VA, such as enzymatic hydrolysis, chemical hydrolysis, fermentation extraction, and ultrasonic- or microwave-assisted extraction, have been suggested to improve its biological efficacy [34].

Previous studies have indicated the neuropharmacological activities of proteins obtained from VA extracts, including the regulation of synaptic plasticity, regeneration of motor neurons, and promotion of neurite outgrowth [35]. In addition, VA has exhibited beneficial effects in neurological and neurodegenerative diseases such as ischemia, Alzheimer's disease (AD), and Parkinson's disease (PD). For instance, VA extract ameliorated the

aggregation of Aβ and α-synuclein, which are the major neuropathologies contributing to AD and PD, respectively [36, 37]. Furthermore, VA exerted protective effects against 1-methyl-4-phenyl-1,2,3,6-tetrahydropyridine (MPTP)-induced neurotoxicity by reducing oxidative stress and proinflammatory factors [37]. Therefore, VA has been considered a therapeutic agent for neurodegenerative diseases. Intriguingly, enzymatically digested VA extract more efficiently decreased the Aβ accumulation and Aβ-induced paralysis than cold or hot water VA extract. In addition, the enzymatically digested VA extract primarily comprises substances with lower molecular weights, in contrast to the cold- or hot-water VA extracts with higher molecular weight compounds. Similarly, we found that peptides and proteins were enriched in the enzymatically digested extract of VA compared to YHC-BE-2038, which is a hot water extract of VA (Fig. 1). In addition, YC-1101 demonstrated significant protective effects against mitochondrial dysfunction in LPS- or scopolamine-treated astrocytes. Therefore, the enzymatic digestion method could be extended to extract preparations of other traditional medicines to increase their efficacy.

Although several indicators have been developed and employed to investigate mitochondrial physiology and functions, controversial results of mitochondrial physiology have been reported, such as millimolar-range mitochondrial Ca2+ detection using chameleon or aequorin mutants [38, 39] in contrast to the micromolar-range readings from chelator probes [40]. In addition, each mitochondrial indicator only represents a single mitochondrial characteristic, which limits the explanation of other mitochondrial physiologies. Therefore, our study confirmed the beneficial effects of VA on mitochondrial functions using different indicators of MMP, mitochondrial superoxide, mitochondrial morphology, and their regulatory factors in LPS and scopolamine treatment, which are well-known mitochondrial stressors in astrocytes.

Mitochondria are dynamic organelles that rapidly change their morphology in response to cellular signals that reflect mitochondrial functions, including metabolism, energy levels, stress, and apoptosis. The size and number of mitochondria are primarily regulated by two independent and opposing factors, fission and fusion proteins, which belong to the dynamic GTPase protein family. In addition, fission and fusion factors are essential for controlling the mitochondrial quality. Fission factors segregate and facilitate the elimination of damaged mitochondria [41], whereas fusion factors reduce mitochondrial stress by exchanging contents with adjacent mitochondria [42]. Dynamin-related protein (Drp)1, mitochondrial fission factor (Mff), and mitochondrial fission 1 protein (Fis1) are representative fission factors, and mitofusin (Mfn)1, Mfn2, and optic atrophy (Opa)1 are major fusion factors in mammalian cells [43]. A disruption in the balance between fission and fusion factors results in aberrant mitochondrial morphology and is related to cellular stress, aging, and neurodegenerative diseases. Mutations in the

Drp1 gene are known to block mitochondrial fission and elongate mitochondria by a relative increase in fusion as a normal expression of fusion factors [44]. LPS- and scopolamine-induced mitochondrial fragmentation is linked to mitochondrial dysfunction, such as elevated oxidative stress and reduced ATP production [14]. In the present study, VA largely regulated mitochondrial morphology by reducing fission factors in LPS- and scopolamine-treated astrocytes.

In summary, pretreatment with enzymatically digested VA extract ameliorated the abnormal changes in mitochondrial physiology induced by mitochondrial stressors in primary astrocytes. YC-1101 rescued MMP and repressed mitochondrial superoxide and mitochondrial fragmentation by suppressing fission factors. In addition, YC-1101 contained bioactive low molecular weight of VA peptides and demonstrated better efficacy than hot water extraction. These data suggest that enzymatic digestion has a potently enhancing effect on the mitochondrial function. Altogether, YC-1101 is a promising health functional ingredient in therapeutics and supplemental foods for the treatment of mitochondria-associated neurodegenerative diseases. Furthermore, enzymatic digestion of VA is an efficient method to meet the global demand for VA by improving its biological activities.

Acknowledgments

We thank Dr. Yusuke Ohba (Tom20) and Dr. Gia Voeltz (Drp1 and Mfn2) for providing the plasmids. We also thank Yuhan Care Co., Ltd for providing YC-1101 and YHC-BE-2038.

References

1. Wu FF, Li HQ, Jin LJ, Li XY, Ma YS, You JS, et al. Deer antler base as a traditional Chinese medicine: A review of its traditional uses, chemistry and pharmacology. J Ethnopharmacol. 2013;145(2):403-15. https://doi.org/10.1016/j.jep.2012.12.008

2. Hung YK, Ho ST, Kuo CY, Chen MJ. In vitro effects of velvet antler water extracts from Formosan Sambar deer and red deer on barrier integrity in Caco-2 cell. Int J Med Sci. 2021;18(8):1778-85. https://doi.org/10.7150/ijms.53599

3. Sui ZG, Zhang LH, Huo YS, Zhang YK. Bioactive components of velvet antlers and their pharmacological properties. J Pharmaceut Biomed. 2014;87:229-40. https://doi.org/10.1016/j.jpba.2013.07.044

4. Gilbey A, Perezgonzalez JD. Health benefits of deer and elk velvet antler supplements: a systematic review of randomised controlled studies. The New Zealand medical journal. 2012;125(1367):80-6.

5. Lee SH, Park MH, Park SJ, Kim J, Kim YT, Oh MC, et al. Bioactive Compounds Extracted from Ecklonia cava by Using Enzymatic Hydrolysis Protects High Glucose-Induced Damage in INS-1 Pancreatic beta-Cells. Appl Biochem Biotech. 2012;167(7):1973-85. https://doi.org/10.1007/s12010-012-9695-7

6. Yoo J, Lee J, Zhang M, Mun D, Kang M, Yun B, et al. Enhanced gamma-aminobutyric acid and sialic acid in fermented deer antler velvet and immune promoting effects. J Anim Sci Technol. 2022;64(1):166-82. https://doi.org/10.5187/jast.2021.e132

7. Matias I, Morgado J, Gomes FCA. Astrocyte Heterogeneity: Impact to Brain Aging and Disease. Front Aging Neurosci. 2019;11:59. https://doi.org/10.3389/fnagi.2019.00059

8. De Miranda BR, Rocha EM, Bai Q, El Ayadi A, Hinkle D, Burton EA, Greenamyre JT. Astrocyte-specific DJ-1 overexpression protects against rotenone-induced neurotoxicity in a rat model of Parkinson's disease. Neurobiol Dis. 2018;115:101-14. https://doi.org/10.1016/j.nbd.2018.04.008

9. Ioannou MS, Jackson J, Sheu SH, Chang CL, Weigel AV, Liu H, et al. Neuron-Astrocyte Metabolic Coupling Protects against Activity-Induced Fatty Acid Toxicity. Cell. 2019;177(6):1522-35. https://doi.org/10.1016/j.cell.2019.04.001

10. Morales I, Sanchez A, Puertas-Avendano R, Rodriguez-Sabate C, Perez-Barreto A, Rodriguez M. Neuroglial transmitophagy and Parkinson's disease. Glia. 2020;68(11):2277-99. https://doi.org/10.1002/glia.23839

11. Schousboe A, Bak LK, Waagepetersen HS. Astrocytic Control of Biosynthesis and Turnover of the Neurotransmitters Glutamate and GABA. Frontiers in endocrinology. 2013;4:102. https://doi.org/10.3389/fendo.2013.00102

12. Gobel J, Engelhardt E, Pelzer P, Sakthivelu V, Jahn HM, Jevtic M, et al. Mitochondria-Endoplasmic Reticulum Contacts in Reactive Astrocytes Promote Vascular Remodeling. Cell Metab. 2020;31(4):791-808. https://doi.org/10.1016/j.cmet.2020.03.005

13. Gollihue JL, Norris CM. Astrocyte mitochondria: Central players and potential therapeutic targets for neurodegenerative diseases and injury. Ageing Res Rev. 2020;59. https://doi.org/10.1016/j.arr.2020.101039

14. Jheng HF, Tsal PJ, Guo SM, Rua LH, Chang CS, Su IJ, et al. Mitochondrial Fission Contributes to Mitochondrial Dysfunction and Insulin Resistance in Skeletal Muscle. Mol Cell Biol. 2012;32(2):309-19. https://doi.org/10.1128/Mcb.05603-11

15. Ramirez S, Gomez-Valades AG, Schneeberger M, Varela L, Haddad-Tovolli R, Altirriba J, et al. Mitochondrial Dynamics Mediated by Mitofusin 1 Is Required for POMC Neuron Glucose-Sensing and Insulin Release Control. Cell Metab. 2017;25(6):1390-9. https://doi.org/10.1016/j.cmet.2017.05.010

16. Ishihara N, Fujita Y, Oka T, Mihara K. Regulation of mitochondrial morphology through proteolytic cleavage of OPA1. Embo Journal. 2006;25(13):2966-77. https://doi.org/10.1038/sj.emboj.7601184

17. Ishihara N, Jofuku A, Eura Y, Mihara K. Regulation of mitochondrial morphology by membrane potential, and DRP1-dependent division and FZO1-dependent fusion reaction in mammalian cells. Biochem Bioph Res Co. 2003;301(4):891-8. https://doi.org/10.1016/S0006-291x(03)00050-0

18. Kim SR, Park Y, Li M, Kim YK, Lee S, Son SY, et al. Anti-inflammatory effect of Ailanthus altissima (Mill.) Swingle leaves in lipopolysaccharide-stimulated astrocytes. J Ethnopharmacol. 2022;286:114258. https://doi.org/10.1016/j.jep.2021.114258

19. Suthprasertporn N, Mingchinda N, Fukunaga K, Thangnipon W. Neuroprotection of SAK3 on scopolamine-induced cholinergic dysfunction in human neuroblastoma SH-SY5Y cells. Cytotechnology. 2020;72(1):155-64. https://doi.org/10.1007/s10616-019-00366-7

20. Baek S, Park CI, Hwang YG, Jeon H, Kim S, Song AR, et al. Enzyme-derived deer velvet extract activate the immune response in cyclophosphamide-induced immunosuppressive mice. Food Sci Biotechnol. 2023;32(10):1435-44. https://doi.org/10.1007/s10068-023-01398-8

21. Dong GZ, Jang EJ, Kang SH, Cho IJ, Park SD, Kim SC, Kim YW. Red ginseng abrogates oxidative stress via mitochondria protection mediated by LKB1-AMPK pathway. Bmc Complem Altern M. 2013;13:64. https://doi.org/10.1186/1472-6882-13-64

22. Li L, Du JK, Zou LY, Xia HS, Wu T, Kim Y, Lee Y. The Neuroprotective Effects of Decursin Isolated from Angelica gigas Nakai Against Amyloid beta-Protein-Induced Apoptosis in PC 12 Cells via a Mitochondria-Related Caspase Pathway. Neurochem Res. 2015;40(8):1555-62. https://doi.org/10.1007/s11064-015-1623-0

23. Wang Y, Cao L, Du G. [Protective effects of Aloe vera extract on mitochondria of neuronal cells and rat brain]. Zhongguo Zhong Yao Za Zhi. 2010;35(3):364-8. https://doi.org/10.4268/cjcmm20100324

24. Brogi L, Marchese M, Cellerino A, Licitra R, Naef V, Mero S, et al. beta-Glucans as Dietary Supplement to Improve Locomotion and Mitochondrial Respiration in a Model of Duchenne Muscular Dystrophy. Nutrients. 2021;13(5):1619. https://doi.org/10.3390/nu13051619

25. Huang QX, Li J, Chen JJ, Zhang ZP, Xu P, Qi HY, et al. Ginsenoside compound K protects against cerebral ischemia/reperfusion injury via Mul1/Mfn2-mediated mitochondrial dynamics and bioenergy. J Ginseng Res. 2023;47(3):408-19. https://doi.org/10.1016/j.jgr.2022.10.004

26. Hansen ME, Simmons KJ, Tippetts TS, Thatcher MO, Saito RR, Hubbard ST, et al. Lipopolysaccharide Disrupts Mitochondrial Physiology in Skeletal Muscle Via Disparate Effects on Sphingolipid Metabolism. Shock. 2015;44(6):585-92. https://doi.org/10.1097/Shk.0000000000000468

27. Wong-Guerra M, Jimenez-Martin J, Pardo-Andreu GL, Fonseca-Fonseca LA, Souza DO, de Assis AM, et al. Mitochondrial involvement in memory impairment induced by scopolamine in rats. Neurol Res. 2017;39(7):649-59. https://doi.org/10.1080/01616412.2017.1312775

28. Pendergrass W, Wolf N, Poot M. Efficacy of MitoTracker Green (TM) and CMXRosamine to measure changes in mitochondrial membrane potentials in living cells and tissues. Cytom Part A. 2004;61a(2):162-9. https://doi.org/10.1002/cyto.a.20033

29. Indo HP, Yen HC, Nakanishi I, Matsumoto K, Tamura M, Nagano Y, et al. A mitochondrial superoxide theory for oxidative stress diseases and aging. J Clin Biochem Nutr. 2015;56(1):1-7. https://doi.org/10.3164/jcbn.14-42

30. Robinson KM, Janes MS, Beckman JS. The selective detection of mitochondrial superoxide by live cell imaging. Nat Protoc. 2008;3(6):941-7. https://doi.org/10.1038/nprot.2008.56

31. Yamamoto H, Itoh N, Kawano S, Yatsukawa Y, Momose T, Makio T, et al. Dual role of the receptor Tom20 in specificity and efficiency of protein import into mitochondria. Proc Natl Acad Sci U S A. 2011;108(1):91-6. https://doi.org/10.1073/pnas.1014918108

32. Kashiwagi S, Fujioka Y, Satoh AO, Yoshida A, Fujioka M, Nepal P, et al. Folding Latency of Fluorescent Proteins Affects the Mitochondrial Localization of Fusion Proteins. Cell Struct Funct. 2019;44(2):183-94. https://doi.org/DOI 10.1247/csf.19028

33. Echave J, Fraga-Corral M, Garcia-Perez P, Popovic-Djordjevic J, Avdovic EH, Radulovic M, et al. Seaweed Protein Hydrolysates and Bioactive Peptides: Extraction, Purification, and Applications. Mar Drugs. 2021;19(9):500. https://doi.org/10.3390/md19090500

34. Xia PJ, Liu DY, Jiao YY, Wang ZG, Chen X, Zheng S, et al. Health Effects of Peptides Extracted from Deer Antler. Nutrients. 2022;14(19):4183. https://doi.org/10.3390/nu14194183

35. Li CH, Sun YN, Yang WF, Ma SH, Zhang LL, Zhao J, et al. Pilose Antler Extracts (PAEs) Protect against Neurodegeneration in 6-OHDA-Induced Parkinson's Disease Rat Models. Evid-Based Compl Alt. 2019;2019:7276407. https://doi.org/10.1155/2019/7276407

36. Du FZ, Zhao HP, Yao MJ, Yang YY, Jiao JX, Li CY. Deer antler extracts reduce amyloid-beta toxicity in a Caenorhabditis elegans model of Alzheimer's disease. J Ethnopharmacol. 2022;285:114850. https://doi.org/10.1016/j.jep.2021.114850

37. Liu Y, Li HY, Li YF, Yang M, Wang XH, Peng YH. Velvet Antler Methanol Extracts Ameliorate Parkinson's Disease by Inhibiting Oxidative Stress and Neuroinflammation: From C. elegans to Mice. Oxid Med Cell Longev. 2021;2021:8864395. https://doi.org/10.1155/2021/8864395

38. Montero M, Alonso MT, Carnicero E, Cuchillo-Ibanez I, Albillos A, Garcia AG, et al. Chromaffin-cell stimulation triggers fast millimolar mitochondrial Ca2+ transients that modulate secretion. Nat Cell Biol. 2000;2(2):57-61. https://doi.org/Doi 10.1038/35000001

39. Arnaudeau S, Kelley WL, Walsh JV, Demaurex N. Mitochondria recycle Ca2+ to the endoplasmic reticulum and prevent the depletion of neighboring endoplasmic reticulum regions. J Biol Chem. 2001;276(31):29430-9. https://doi.org/DOI 10.1074/jbc.M103274200

40. Drummond RM, Mix TCH, Tuft RA, Walsh JV, Fay FS. Mitochondrial Ca2+ homeostasis during Ca2+ influx and Ca2+ release in gastric myocytes from Bufo marinus. J Physiol. 2000;522(3):375-90. https://doi.org/DOI 10.1111/j.1469-7793.2000.t01-2-00375.x

41. Ding WX, Yin XM. Mitophagy: mechanisms, pathophysiological roles, and analysis. Biol Chem. 2012;393(7):547-64. https://doi.org/10.1515/hsz-2012-0119

42. Liu XG, Weaver D, Shirihai O, Hajnoczky G. Mitochondrial 'kiss-and-run': interplay between mitochondrial motility and fusion-fission dynamics. Embo Journal. 2009;28(20):3074-89. https://doi.org/10.1038/emboj.2009.255

43. Liu YJ, McIntyre RL, Janssens GE, Houtkooper RH. Mitochondrial fission and fusion: A dynamic role in aging and potential target for age-related disease. Mech Ageing Dev. 2020;186:111212. https://doi.org/10.1016/j.mad.2020.111212

44. Smirnova E, Griparic L, Shurland DL, van der Bliek AM. Dynamin-related protein Drp1 is required for mitochondrial division in mammalian cells. Mol Biol Cell. 2001;12(8):2245-56. https://doi.org/10.1091/mbc.12.8.2245

Figure legends

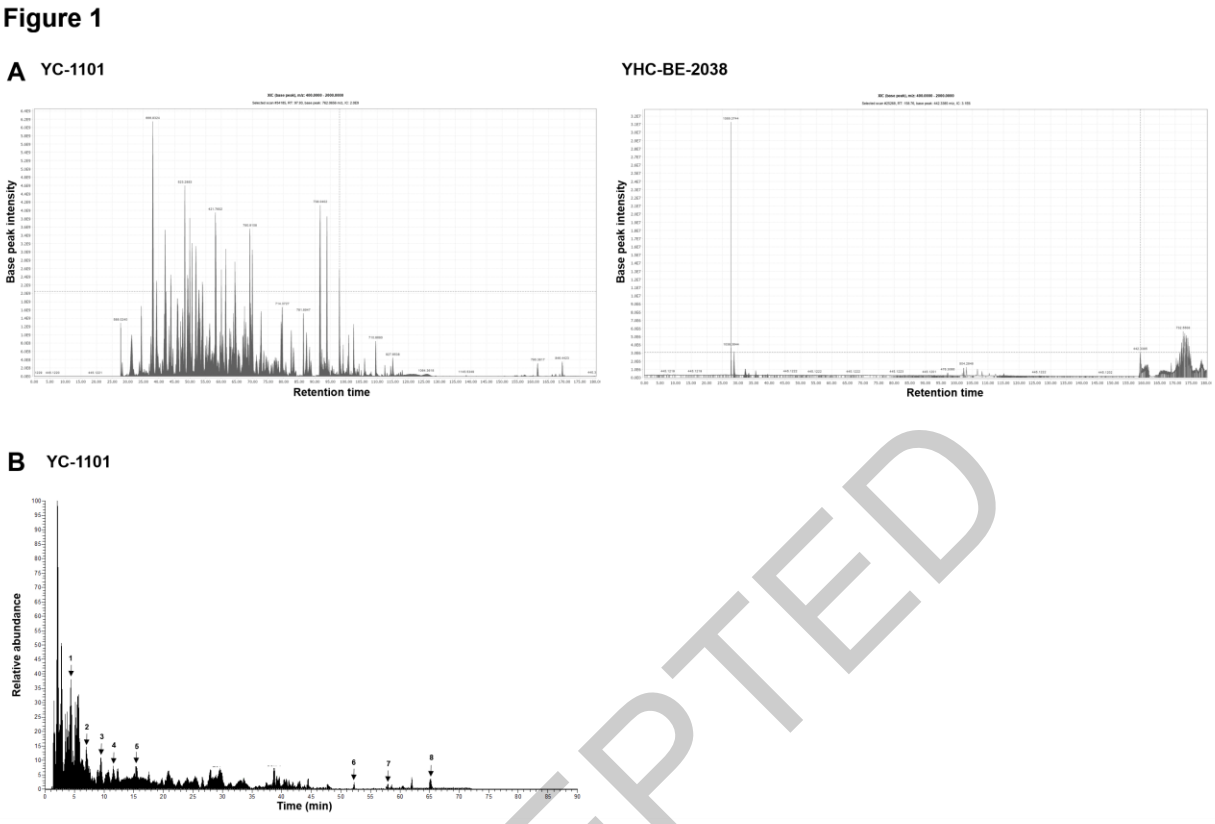

Fig. 1. LC-MS/MS total ion chromatogram and representative structures detected in YC-1101.

(A) Total ion chromatogram of YC-1101 and YHC-BE-2038. (B) 1; Leu-Val, 3'-Adenosine monophosphate (3'-AMP), 3-(1-hydroxyethyl)-2,3,6,7,8,8a-hexahydropyrrolo[1,2-a]pyrazine-1,4-dione, 2-([4-(Benzyloxy)anilino]carbonylamino)-N-(3-morpholinopropyl)benzamide, (Ac)2-L-Lys-D-Ala, Fasoracetam. 2; Leu-Leu, Pyridoxamine. 3; Troxipide. 4; Ophthalmic acid. 5; 1-O-[(3β,5ξ,9ξ)-3-[6-Deoxy-α-L-mannopyranosyl-(1->4)-[β-D-galactopyranosyl-(1->2)]-β-D-glucopyranuronosyl]oxy-28-oxoolean-12-en-28-yl]-β-D-glucopyranose. 6; Nitrendipine. 7; NP-013663, 5-trans prostaglandin F2β, A-12(13)-EpODE, Stearidonic acid, (12Z)-9,10,11-trihydroxyoctadec-12-enoic acid, 6,7,8-trimethoxy-3-phenyl-2-thioxo-1,2,3,4-tetrahydroquinazolin-4-one, 1,4-Bis(cyclohexylamino)-9,10-anthraquinone, (+/-)8-HEPE, Dodecyltrimethylammonium. 8; 2,3-Dihydroxypropyl stearate.

Figure 2

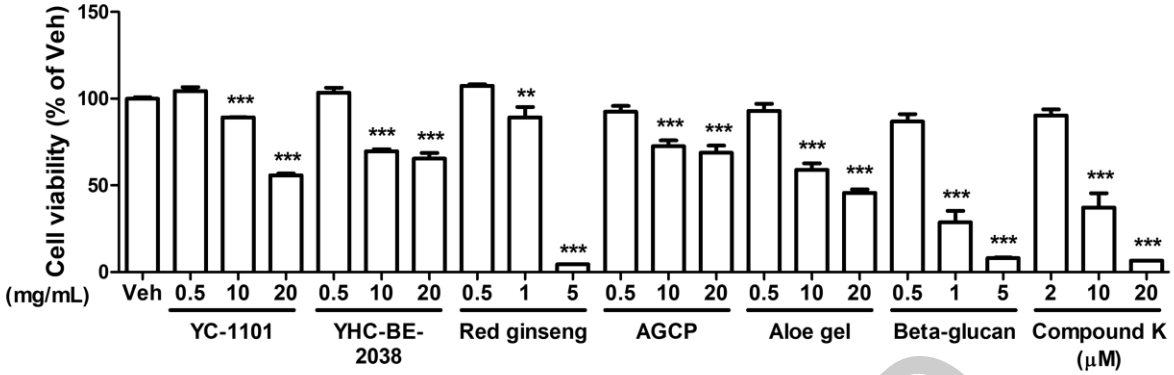

Fig. 2. Effects of YC-1101 on cell viability in primary cultured astrocytes.

Astrocytes were treated with each compound for 24 h, and viability was determined using the MTT assay. Data are presented as the mean ± standard error of the mean (SEM) and were analyzed for statistical significance using one-way analysis of variance (ANOVA) followed by a post hoc Tukey's test. Statistical significance was set at $p<0.05$.

Figure 3

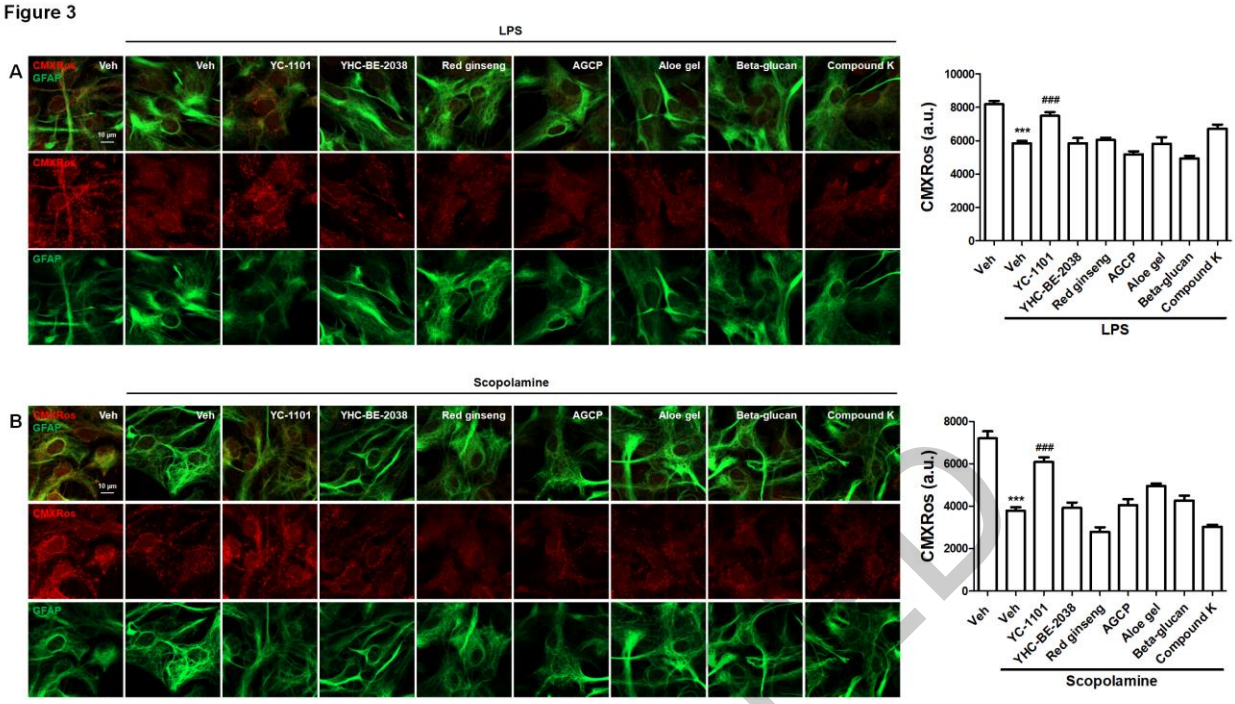

Fig. 3. Effects of YC-1101 on mitochondrial membrane potential in LPS- or scopolamine-treated astrocytes. The astrocytes were treated with the compounds for 1 h and further incubated with LPS or scopolamine for 24 h. After incubation, CMXRos was used to detect MMP, and the cells were fixed for immunostaining. GFAP was used as an astrocyte marker. Representative images and quantification of MMP in astrocytes. (A) Effects of the compounds on LPS-induced depolarization of MMP. YC-1101 attenuates LPS-induced MMP depolarization (B) Scopolamine treatment, as in Panel A. Data are presented as the mean ± SEM. Student's t-test. ***$p<0.001$ as compared with the Veh, ###$p<0.001$ as compared with the Veh + LPS or scopolamine. Scale bar = 10 μm.

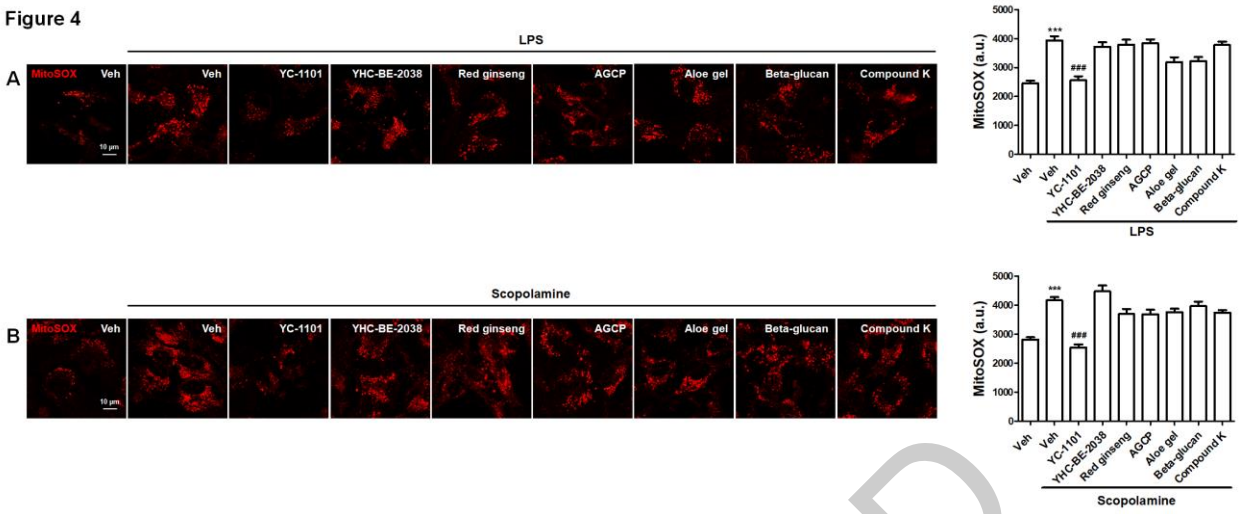

Fig. 4. Effects of YC-1101 on mitochondrial superoxide in LPS- or scopolamine-treated living astrocytes. At the end of treatment, astrocytes were incubated with MitoSOX to measure mitochondrial superoxide levels. Images of MitoSOX were captured in living astrocytes. Representative images and quantification of MitoSOX expression. (A) YC-1101 ameliorated the LPS-induced elevation of mitochondrial superoxide activity. (B) Similar to panel A but treated with scopolamine. Data are presented as the mean ± SEM. Student's t-test. ***$p<0.001$ as compared with the Veh, ###$p<0.001$ as compared with the Veh + LPS or scopolamine. Scale bar = 10 μm.

Figure 5

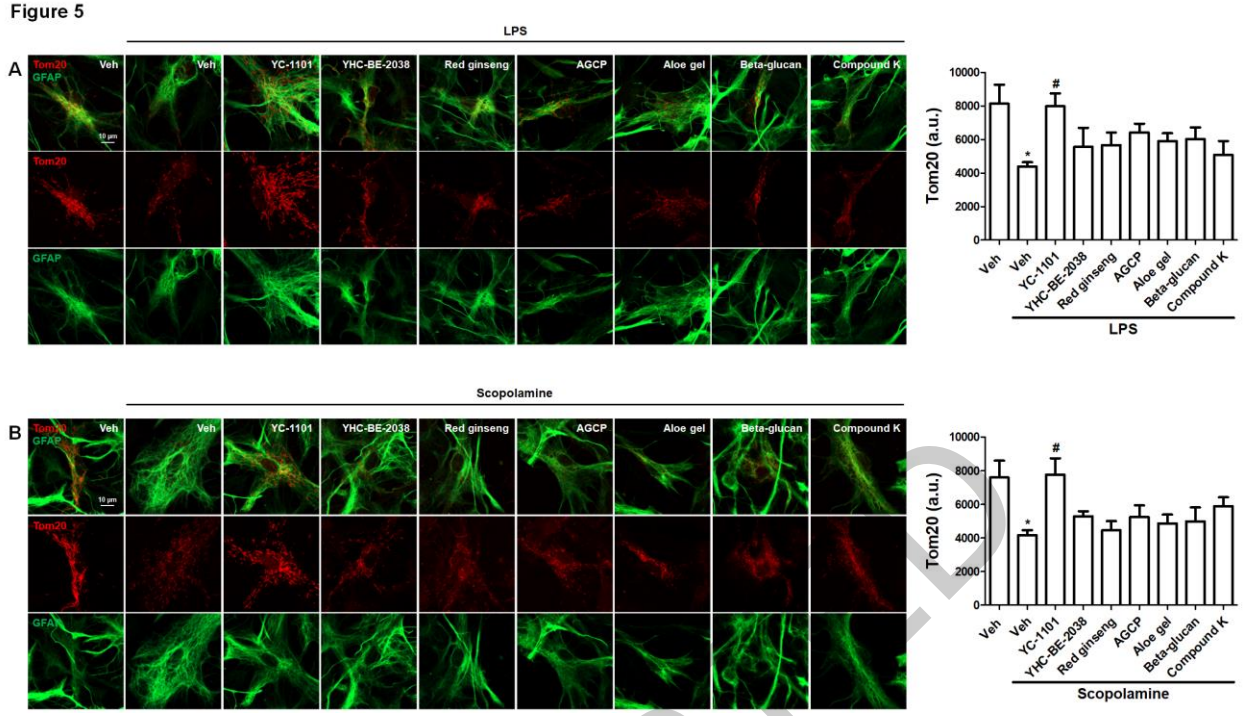

Fig. 5. Effects of YC-1101 on mitochondrial fragmentation in LPS- or scopolamine-treated astrocytes. Astrocytes were transfected with Tom20 to visualize mitochondrial morphology and treated with LPS or scopolamine. At the end of the treatment, images of Tom20 in living astrocytes were captured. Representative images and quantification of Tom20 expression. (A and B) YC-1101 attenuated mitochondrial fragmentation induced by LPS or scopolamine. Data are presented as the mean ± SEM. Student's t-test. *$p<0.05$, compared to Veh; #$p<0.05$, compared to Veh + LPS or scopolamine. Scale bar = 10 μm.

Figure 6

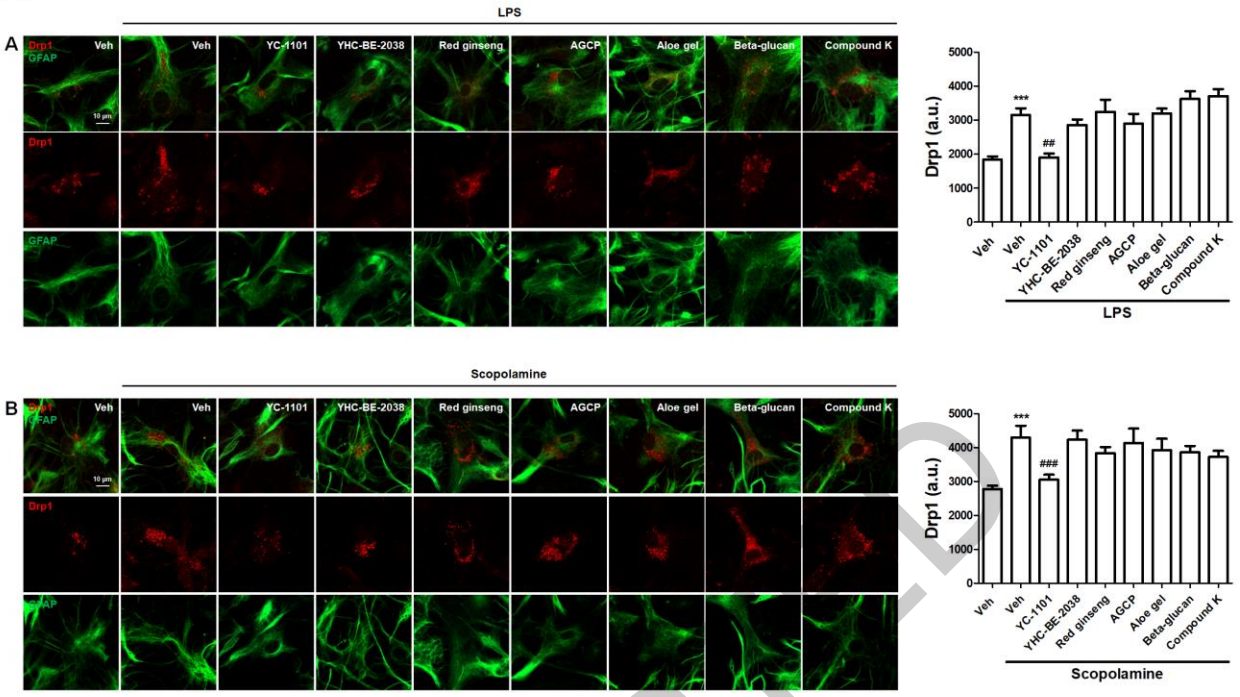

Fig. 6. Effects of YC-1101 on Drp1 expression in LPS- or scopolamine-treated astrocytes.

Drp1 transfection in astrocytes was followed by treatment with LPS or scopolamine. Drp1 images were captured from living astrocytes. Representative images and quantification of Drp1 expression. (A and B) YC-1101 restored Drp1 expression following LPS or scopolamine treatment. Data are presented as the mean ± SEM. Student's t-test. **p<0.01 as compared with the Veh, ##p<0.01 as compared with the Veh + LPS or scopolamine. Scale bar = 10 μm.

Figure 7

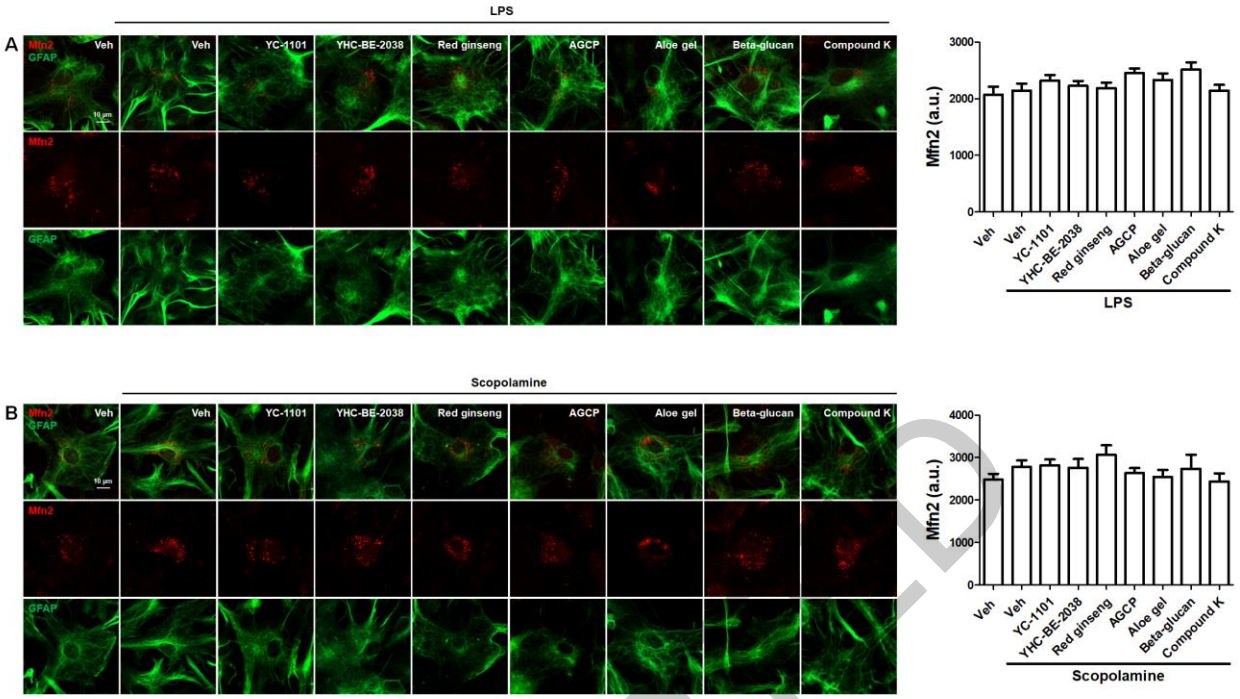

Fig. 7. Effects of YC-1101 on Mfn2 expression in LPS- or scopolamine-treated astrocytes.

As shown in Fig. 7, Mfn2 is expressed in astrocytes. Representative images and quantification of Mfn2 expression. (A and B) LPS or scopolamine treatment induced marginal changes in the Mfn2 expression in astrocytes compared with the Veh group. Mfn2 expression was similar in all the groups. Data are presented as the mean ± SEM. Student's t-test. Scale bar = 10 μm.

508 **Table 1. Identification of metabolites in YC-1101 using LC-MS/MS**

	Name	Formula	MW[a]	RT[b] (min)	Area (Max.)	MS²
	Leu-Val	$C_{11}H_{22}N_2O_3$	230.16	4.388	9248335356	DDA[c] for preferred ion
	3'-Adenosine monophosphate (3'-AMP)	$C_{10}H_{14}N_5O_7P$	347.06	4.372	864964131	DDA for preferred ion
1	3-(1-Hydroxyethyl)-2,3,6,7,8,8a-hexahydropyrrolo[1,2-a]pyrazine-1,4-dione	$C_9H_{14}N_2O_3$	198.10	4.392	183176888.2	DDA for preferred ion
	2-([4-(Benzyloxy)anilino]carbonylamino)-N-(3-morpholinopropyl)benzamide	$C_{28}H_{32}N_4O_4$	244.11	4.398	81541554.31	DDA for other ion
	(Ac)2-L-Lys-D-Ala	$C_{13}H_{23}N_3O_5$	301.16	4.487	72810363.32	DDA for preferred ion
	Fasoracetam	$C_{10}H_{16}N_2O_2$	196.12	4.346	45985786.28	No MS2
2	Leu-Leu	$C_{12}H_{24}N_2O_3$	244.17	6.959	589975860.4	DDA for preferred ion
	Pyridoxamine	$C_8H_{12}N_2O_2$	168.08	7.028	56050776.08	DDA for preferred ion
3	Troxipide	$C_{15}H_{22}N_2O_4$	294.15	9.411	360973783.8	No MS2
4	ophthalmic acid	$C_{11}H_{19}N_3O_6$	289.12	11.611	565971241.3	DDA for preferred ion
5	1-O-[(3β,5ξ,9ξ)-3-[6-Deoxy-α-L-mannopyranosyl-(1->4)-[β-D-galactopyranosyl-(1->2)]-β-D-glucopyranuronosyl]oxy-28-oxoolean-12-en-28-yl]-β-D-glucopyranose	$C_{54}H_{86}O_{23}$	1124.52	15.447	5040660497	DDA for preferred ion
6	Nitrendipine	$C_{18}H_{20}N_2O_6$	360.13	52.245	308626777.7	DDA for other ion
	NP-013663	$C_{18}H_{34}O_5$	352.22	57.953	205483034.7	DDA for preferred ion
	5-Trans prostaglandin F2β	$C_{20}H_{34}O_5$	376.22	57.914	144312489.6	DDA for preferred ion
	A-12(13)-EpODE	$C_{18}H_{30}O_3$	294.21	57.981	100950027.2	No MS2
	Stearidonic acid	$C_{18}H_{28}O_2$	276.20	58.026	98917118.98	DDA for preferred ion
7	(12Z)-9,10,11-Trihydroxyoctadec-12-enoic acid	$C_{18}H_{34}O_5$	312.22	57.952	72851922.93	DDA for preferred ion
	6,7,8-Trimethoxy-3-phenyl-2-thioxo-1,2,3,4-tetrahydroquinazolin-4-one	$C_{17}H_{16}N_2O_4S$	344.07	57.934	57223133.62	DDA for preferred ion
	1,4-Bis(cyclohexylamino)-9,10-anthraquinone	$C_{26}H_{30}N_2O_2$	402.23	58.054	46035476.28	DDA for preferred ion
	(+/-)8-HEPE	$C_{20}H_{30}O_3$	300.20	57.885	31656498.53	DDA for preferred ion
	Dodecyltrimethylammonium	$C_{15}H_{33}N$	227.26	57.941	29874524.83	DDA for preferred ion

8	2,3-Dihydroxypropyl stearate	$C_{21}H_{42}O_4$	358.30	65.132	1094633983	DDA for other ion

[a]Molecular weight.
[b]Retention time.
[c]Data-dependent acquisition.